Tuning Strain and Quality Factor of 2D MoS_2 NEMS Resonators using Annealing and Electrostatic Gating

Pengcheng Zhang[1], Yueyang Jia[1], Zuheng Liu[1], and Rui Yang[1,2*]
[1]University of Michigan–Shanghai Jiao Tong University Joint Institute,
Shanghai Jiao Tong University, Shanghai, China
[2]School of Electronic Information and Electrical Engineering,
Shanghai Jiao Tong University, Shanghai 200240, China
[*]Email: rui.yang@sjtu.edu.cn

***Summary*—We develop a technique for wide-range tuning of strain and quality (Q) factor in resonant two-dimensional (2D) molybdenum disulfide (MoS_2) nanoelectromechanical systems (NEMS), by using thermal annealing combined with electrostatic gating. The initial strains of three fully-clamped circular MoS_2 NEMS resonators are released by a thermal annealing process, and their resonances under different DC gate voltages (V_{GS}) before and after annealing are measured. We find that the annealed devices have smaller initial strains, corresponding to smaller eigenfrequencies and wider frequency tuning ranges. We further extract the Q for these MoS_2 resonators before and after annealing. The results show that Q increases with V_{GS} in both the annealed and non-annealed cases, and the annealed devices have a smaller initial Q and a larger Q tuning range. By varying V_{GS}, we can tune the Q for fully-clamped resonators by $\Delta Q/Q$ = 528.3% before annealing and by $\Delta Q/Q$ = 891.7% after annealing. This strain dependence of Q is important for optimizing sensitivity, dynamic range, and signal transduction efficiency of 2D NEMS resonators towards ultralow-power, ultra-sensitive and frequency-selective devices for sensing, memory, computing, and signal processing.**

Keywords*—MoS_2; 2D NEMS resonator; Q factor; annealing; Strain tuning

I. INTRODUCTION

NEMS resonators based on 2D semiconductors such as MoS_2 attract increasing attention, for transducing external stimuli with ultrahigh sensitivity towards the quantum limit [1], a broad dynamic range (up to ~70 to 110 dB) [2], and a large frequency tuning range (up to 1300%) [3]. Q factor plays a critical role in these NEMS resonators [4], because important device parameters such as the frequency selectivity, dissipation, sensitivity, and dynamic range are all tunable by Q. For example, the sensitivity of force sensors and frequency selectivity for radio-frequency (RF) filters improve with a higher Q [5,6]; the dynamic range increases with a lower Q [7]. Therefore, a reliable technique for tuning Q can allow optimizing the single NEMS resonator for different sensing or RF signal processing applications. Different from bulk microelectromechanical systems (MEMS), in atomically-thin 2D NEMS resonators the frequency, Q and many other important device properties are extremely sensitive to stress or strain [8–10]. But the effects of initial strain on device performance, and a technique for tuning Q with a broad range, are still under exploration.

Here, we measure the annealing effect on strain and Q of three fully-clamped circular 2D MoS_2 NEMS resonators, and perform tuning of strain and Q by varying V_{GS}. The thermal annealing releases the initial strain, as shown by smaller initial eigenfrequencies at V_{GS} = 0 V, and broader frequency tuning ranges. Besides, smaller initial strains in these MoS_2 NEMS resonators also make the Q more effectively tuned by V_{GS}, with $\Delta Q/Q$ of 528.3% before annealing and $\Delta Q/Q$ up to 891.7% after annealing. Such broad tuning range of Q can enable ultrasensitive and large-dynamic-range transducers, tunable RF front end for efficient signal processing, or computing devices.

II. RESULTS AND DISCUSSIONS

The fabrication starts with preparation of the substrate, by patterning local back gates, growing isolation oxide layer using plasma-enhanced chemical vapor deposition, etching surface circular microtrenches, and patterning surface contact electrodes. Then MoS_2 membrane is mechanically exfoliated onto a polymer stamp and transferred onto the circular microtrench (Fig. 1a), by using a dry-transfer technique [11].

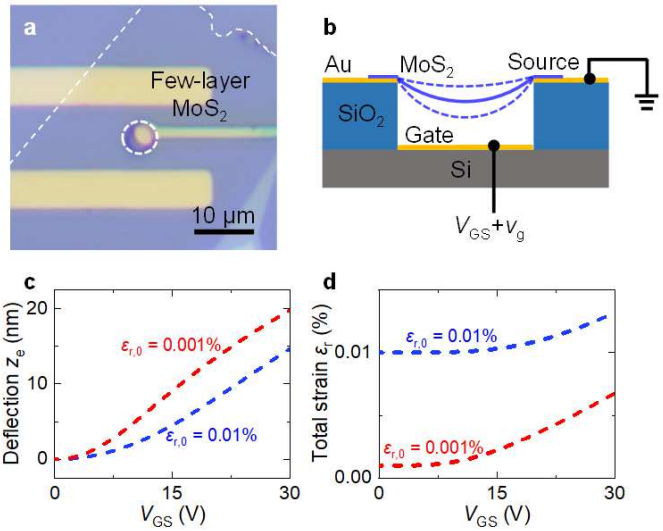

Fig. 1. Fully-clamped circular 2D MoS_2 NEMS resonator device structure and calculated static characteristics varying with DC gate voltage V_{GS} at different initial strains. (a) Optical image of a few-layer fully-clamped circular resonator as shown by the white dashed circle. *Scale bar*: 10 μm. (b) Cross-sectional illustration of the device motion, where the source electrode is grounded and the gate electrode is under an electrcial drive through a bias tee. (c) Calculated static deflection z_e varying with V_{GS} at different initial strains. The red dashed line is for initial strain of 0.001%, and the blue dashed line is for intial strain of 0.01%. (d) Calculated total strain varying with V_{GS} at different initial strains.

As shown in Fig. 1b, the motion is excited capacitively using the DC voltage V_{GS} and AC driving voltage v_g applied at the local gate through a bias tee, with the source grounded. V_{GS} can deflect the suspended MoS_2 membrane by displacement z_e which is solved by the equilibrium of the elastic and electrostatic forces. This will then induce a DC tensile strain ε_r, which can be calculated as [12]:

$$\varepsilon_r = \frac{1+\varepsilon_{0,r}}{2R}\int_{-R}^{R}\sqrt{1+\left(\frac{\partial w}{\partial r}\right)^2}\,dr - 1, \qquad (1)$$

where $\varepsilon_{0,r}$ is the initial strain, R is the radius and $w(r) = z_e((R^2-r^2)/R^2)^2$ is the deflection profile. We calculate the static deflection and strain induced by V_{GS}, at initial strains of 0.01% and 0.001%. We find that device with a smaller initial strain has a larger static deflection at the same V_{GS}, *i.e.*, V_{GS}-induced deflection z_e reaches 20 nm at V_{GS} = 30 V when $\varepsilon_{0,r}$ is 0.001%, while z_e is 15 nm at V_{GS} = 30 V for the device with $\varepsilon_{0,r}$ of 0.01% (Fig. 1c). Therefore, the device with a smaller initial strain has a larger V_{GS} tuning range of total strain up to 575.8% (Fig. 1d). The device motion is detected by using a custom-built optical interferometry system [8].

To release the initial strain in 2D MoS_2 NEMS resonators, we use a tube furnace system to conduct thermal annealing in nitrogen gas (N_2) environment under atmosphere pressure. We first place the substrate with devices in the quartz tube with N_2 flow, and then the temperature is gradually increased to 300 °C with an increasing rate of 9 °C per minute. After 30 minutes of preserving the temperature at 300 °C, the furnace is naturally cooled down to room temperature in about 120 minutes.

We first measure the resonances of a 2D MoS_2 NEMS resonator noted as Device 1 (Fig. 1a) before thermal annealing, with varying V_{GS} (Fig. 2a). The resonance frequency increases from 19.7 MHz to 22 MHz, and $\varepsilon_{0,r}$ (at V_{GS} = 0 V) of 0.048% is extracted through fitting to the frequency tuning characteristics. Besides, the frequency tuning characteristics of another two 2D MoS_2 NEMS resonators before annealing are also measured, for which the resonance frequencies increase from 10.5 MHz to 13.7 MHz for Device 2 (Fig. 2c), and from 19.1 MHz to 26.3 MHz for Device 3 (Fig. 2e). The initial strains of 0.01% for Device 2, and 0.017% for Device 3 are extracted through fitting to the frequency tuning characteristics.

Then we anneal all the three devices to release the initial strain *via* our thermal annealing process, measure their resonances, and fit the frequency tuning characteristics to extract the initial strains (Fig. 2b, 2d and 2f). We find that the initial eigenfrequencies decrease, and the frequency tuning ranges with the same V_{GS} range increase a lot after annealing. This is because that the resonant frequency f_{res} of the 2D NEMS resonators is highly dependent on strain or stress, which can be modeled by [8]:

$$f_{res} = \frac{1}{2\pi}\sqrt{\frac{2.405^4 E_Y \varepsilon_r}{2\rho R^2} - \frac{\kappa}{0.75\rho t g^3}V_{GS}^2}, \qquad (2)$$

where t, ρ, E_Y, R, g, and κ are the thickness, mass density, Young's modulus, radius, initial vacuum gap, and vacuum permittivity of the MoS_2 device, respectively.

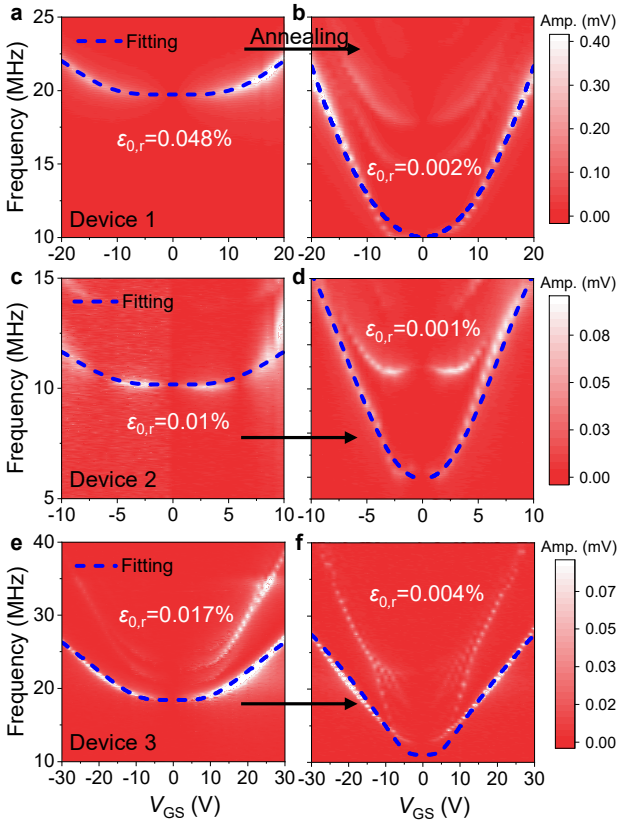

Fig. 2. The measured frequency tuning for three MoS_2 drumhead resonators before and after annealing, with the amplitude shown in color scale. The initial strains of (a) 0.048% before annealing and (b) 0.002% after annealing are extracted by fitting to the frequency tuning for Device 1, where the blue dashed lines are the model fitting. Similarly, the initial strains of (c) 0.01% before and (d) 0.001% after annealing for Device 2, and (e) 0.017% before and (f) 0.004% after annealing for Device 3 are extracted.

For Device 1 in Fig. 2a–2b, its resonant frequency f_0 at V_{GS} = 0 V decreases from 19.7 MHz before annealing to 10.02 MHz after annealing, and the frequency tuning range $\Delta f/f_0$ increases dramatically from 11.7% to 123.5%. We extract the initial strains from fitting to the frequency tuning characteristics, and find that for all three devices, the initial strains significantly decrease after annealing, from 0.048%, 0.01%, and 0.017% down to 0.002%, 0.001%, and 0.004% for Devices 1, 2, and 3, respectively. The f_0 are all smaller after annealing, with f_0 down to 6.1 MHz for Device 2 (Fig. 2c–2d) and 12.5 MHz for Device 3 (Fig. 2e–2f), because smaller initial strains lower the f_0. The frequency tuning ranges are all larger after annealing, with $\Delta f/f_0$ up to 146.8% for Device 2 and 120% for Device 3, which shows larger V_{GS}-induced strains.

The strains can also tune the Q in these 2D MoS_2 drumhead NEMS resonators, which can be modeled as [8]:

$$Q^{-1} = \frac{5.576\delta z^2(V_{GS})}{\varepsilon_r(V_{GS})R^2(1-\nu^2)}\,\delta_{elong} + Q_{other}^{-1}, \qquad (3)$$

where δz, ν, δ_{elong} and Q_{other}^{-1} are the vibration amplitude, Poisson's ratio, loss angle, and dissipation from other driving-force-independent mechanisms, respectively. As shown in Fig. 3a, we extract the Q for Device 1 before (Fig. 3a) and after annealing (Fig. 3c) at V_{GS} = 15 V, where Q of 41 and 35.6 are

extracted before and after annealing, respectively. This is because a larger tensile strain before annealing can lead to smaller thermoelastic damping and thus a higher Q as demonstrated in Eq. 3. Then the Q factors at different V_{GS} are summarized in Fig. 3b and 3d, showing that the Q before annealing can be tuned from 35.1 to 53.6 (Fig. 3b), corresponding to $\Delta Q/Q$ = 52.7%, and the Q factors after annealing show a larger tuning range from 30.7 to 52.3, corresponding to $\Delta Q/Q$ = 70.4%. This is consistent with the results from the frequency tuning, which show a larger strain range, and thus can lead to a larger Q tuning range.

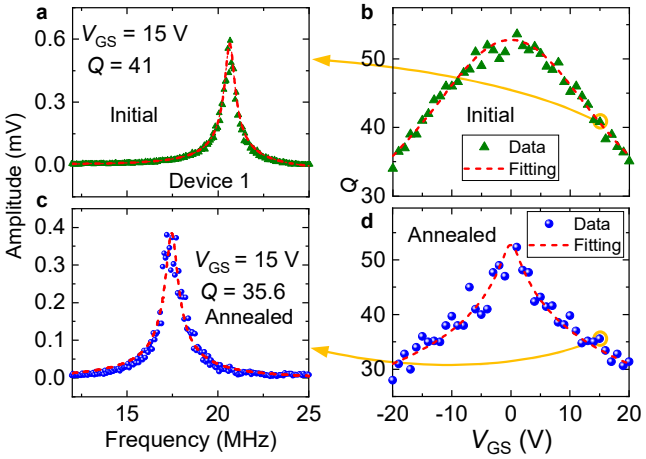

Fig. 3. Summary of Q for the 2D MoS_2 NEMS resonator in Fig. 1a (Device 1). (a–d) Measured resonances at different V_{GS} and the dependence of Q on V_{GS} (a–b) before annealing, and (c–d) after annealing, at v_g = 50 mV. The Q at V_{GS} = 15 V decreases after annealing, from (a) 41 to (c) 35.6. The green triangles and blue symbols are the experimental data obtained before and after annealing, respectively, and the red dashed lines show the model fitting.

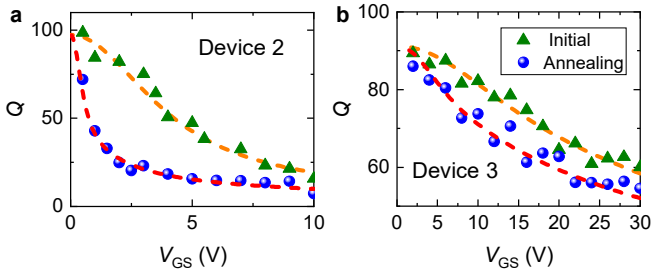

Fig. 4. Summary of Q for (a) Device 2 and (b) Device 3. The green triangles and blue symbols are the experimental data obtained before and after annealing, respectively, and the red dashed lines show the model fitting.

TABLE I. Comparison of device performance before and after annealing.

	Initial			After Annealing		
Device (#)	***Initial strain***	***Δf/f₀***	***ΔQ/Q***	***Initial strain***	***Δf/f₀***	***ΔQ/Q***
1	0.048%	11.7%	52.7%	0.002%	123.5%	70.4%
2	0.01%	14.6%	528.3%	0.001%	146.8%	891.7%
3	0.017%	42.3%	50.1%	0.004%	145.7%	57.5%

Similarly, we measure and summarize the Q with varying V_{GS} before and after annealing, for the other two devices (Fig. 4), showing that $\Delta Q/Q$ increases from 528.3% to 891.7% for Device 2, and from 50.1% to 57.5% for Device 3. The detailed comparison of characteristics before and after annealing for all three devices are summarized in Table I. In general, after the annealing process, the initial strains decrease, and the V_{GS} tuning ranges increase for both resonance frequency and Q.

III. Conclusions

In summary, we have measured the resonances and extracted the Q for three MoS_2 NEMS resonators before and after thermal annealing. Their initial eigenfrequencies and Q at V_{GS} = 0 V always decrease after annealing, while both the frequency and Q have larger V_{GS} tuning ranges due to released initial strains. The results are important for optimizing the Q factors for 2D NEMS resonators towards new types of sensing, RF signal processing, memory, and computing devices.

Acknowledgment

The authors thank the support from National Natural Science Foundation of China (NSFC) (Grants 62250073, 62104140, U21A20505), Science and Technology Commission of Shanghai Municipality (STCSM) Shanghai Rising-Star Program (Grant 23QA1405300) and Natural Science Project General Program (Grant 21ZR1433800), Lingang Laboratory Open Research Fund (Grant LG-QS-202202-11), and Biren Technology–Shanghai Jiao Tong University Joint Laboratory Open Research Fund. The authors thank the Center for Advanced Electronic Materials and Devices (AEMD) of Shanghai Jiao Tong University, for the support in the fabrication and measurements of the devices.

References

[1] A. Bachtold, *et al.* "Mesoscopic physics of nanomechanical systems." Rev. Mod. Phys., vol. 94, 045005, 2022.

[2] J. Lee, *et al.* "Electrically tunable single- and few-layer MoS_2 nanoelectromechanical systems with broad dynamic range." Sci. Adv., vol. 4, eaao6653, 2018.

[3] F. Ye, *et al.,* "Glowing graphene nanoelectromechanical resonators at ultra-high temperature up to 2650K." Tech. Digest IEDM'18, pp. 87-90, 2018.

[4] B. Xu, *et al.*, "Nanomechanical resonators: toward atomic scale." ACS Nano, vol. 16, pp. 15545-15585, 2022.

[5] C. Chen, *et al.*, "Graphene mechanical oscillators with tunable frequency." Nat. Nanotechnol., vol. 8, pp. 923-927, 2013.

[6] R. Yang, *et al.*, "6H-SiC microdisk torsional resonators in a "smart-cut" technology." Appl. Phys. Lett., vol. 104, 091906, 2014.

[7] Z. Wang, *et al.*, "Dynamic range of atomically thin vibrating nanomechanical resonators." Appl. Phys. Lett., vol. 104, 103109, 2014.

[8] P. Zhang, *et al.*, "Strain-modulated dissipation in two-dimensional molybdenum disulfide nanoelectromechanical resonators." ACS Nano, vol. 2, pp. 2261-2270, 2022.

[9] P. Zhang, *et al.*, "Strain-modulated equivalent circuit model and dissipation model for 2D MoS_2 NEMS resonators." in Proc. MEMS'21 Conference, pp. 658–661, 2021.

[10] R. Yang, A. Islam, P. X.-L. Feng, "Electromechanical coupling and design considerations in single-layer MoS_2 suspended-channel transistors and resonators." Nanoscale, vol. 7, pp. 19921–19929, 2015.

[11] R. Yang, *et al.*, "Multilayer MoS_2 transistors enabled by a facile dry-transfer technique and thermal annealing." J. Vac. Sci. Technol. B, vol. 6, 061203, 2014.

[12] T. Mei, *et al.* "Frequency tuning of graphene nanoelectromechanical resonators via electrostatic gating." Micromachines, vol. 9, pp. 312, 2018.